PHYSICAL REVIEW B **73**, 241308(R) (2006)

Spatial structure and stability of the macroscopically occupied polariton state in the microcavity optical parametric oscillator

D. Sanvitto,* D. N. Krizhanovskii, D. M. Whittaker, S. Ceccarelli, and M. S. Skolnick
Department of Physics and Astronomy, University of Sheffield, Sheffield S3 7RH, United Kingdom

J. S. Roberts
Department of Electronic and Electrical Engineering, University of Sheffield, Sheffield S1 3JD, United Kingdom
(Received 20 December 2005; revised manuscript received 27 March 2006; published 12 June 2006)

Transverse spatial images of the signal generated in semiconductor microcavities under conditions of resonant parametric scattering are obtained. When the system is pumped significantly above the threshold, the signal image is found to be highly structured, consisting of a set of localized bright spots. By comparison with a numerical model, it is shown that the structure arises from the blueshift generated by the nonlinear polariton-polariton interaction which drives the microcavity optical parametric oscillator, in combination with partially ordered spatial fluctuations in the cavity mode energy. An important outcome is that the form and stability of the signal is strongly influenced by the local cavity disorder.

DOI: 10.1103/PhysRevB.73.241308 PACS number(s): 42.55.Sa, 42.65.Yj, 42.65.Lm, 78.90.+t

Polaritons are quasiparticles arising from the strong interaction between light and optically active excitations of a medium. The light confinement in semiconductor microcavities permits exciton polaritons to be observed and manipulated. New dispersion curves are formed exhibiting very light masses and properties such as bosonic stimulation.[1] Strong nonlinear emission from the bottom of the polariton dispersion is observed under conditions of resonant excitation of the lower polariton branch.[2–4] This arises from optical parametric oscillator (OPO) processes in which two polaritons in the pump state scatter into signal and idler states in a process which conserves energy and momentum (Fig. 1).[5–8] The scattering process leads to a macroscopic occupation of the signal (and idler).

In most of the experimental studies to date, the spatial structure of the signal and idler states has not been investigated, with only quantities such as total power,[2–4] average polarization,[9] or far field (k-space) maps[10,11] reported. Near field images of the reflected pump beam are presented in Refs. 12 and 13. Spatial patterning in the case of nonresonant excitation has also been observed.[14,15] Similarly, in most theoretical treatments, it has been assumed that pump, signal, and idler modes are all plane waves. In reality, this is not the case, because the excitation spot must have finite size that leads to spatial variations in the pump power. In typical experiments, these variations are on a length scale where diffraction (enhanced by the cavity dispersion) is important, so it is not possible to consider the pump as locally uniform. We have recently shown theoretically[16] that the blueshift, due to the polariton-polariton repulsive interaction, tends to switch the OPO off at high pump powers, so this spatial variation in the pump can lead to a highly nonuniform signal spot.

In this work we present spectrally resolved real space images of the OPO signal and explain the observed patterning and stability by comparison with a theoretical model that takes into account finite spot size. In particular, we show that defect induced spatial fluctuations in the cavity photon energy (the "photonic potential"), in combination with energy renormalization of the polariton dispersion, are responsible for polariton localization and stability of the OPO.

The sample studied is a $3\lambda/2$ GaAs microcavity grown by metal-organic chemical-vapor disposition (MOCVD), similar to that in Ref. 3 with Rabi splitting of ~6 meV. The data are collected with the quantum well exciton and the optical mode on resonance at $\mathbf{k}\sim 0$, with the sample immersed in liquid helium at 2 K. A Ti-sapphire laser on resonance with the lower polariton branch at 12° was used to generate the polariton population in the pump state, and the resultant signal and idler populations, as shown in Fig. 1. The signal state is imaged by use of a specially designed wide aperture aspheric lens. The signal is spectrally resolved using an imaging spectrometer to avoid scattered light from the pump beam.

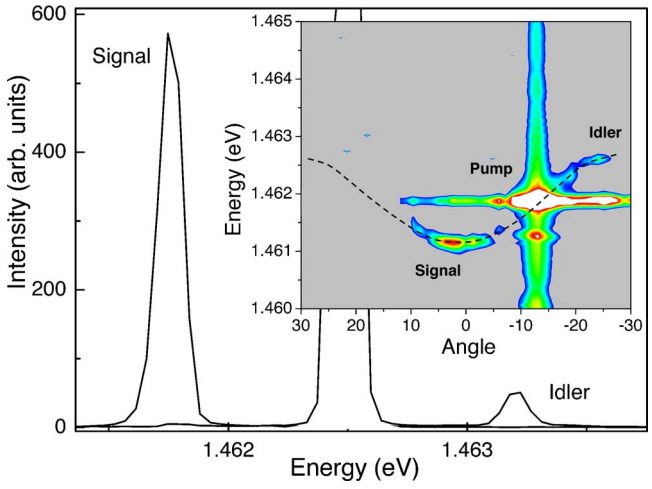

FIG. 1. (Color online) Photoluminescence spectra at $\mathbf{k}\sim 0$ and $\mathbf{k}\sim 2k_p$ for a pump incident at $\mathbf{k}=k_p$ resonant with the lower polariton branch and power 3 times the threshold for the onset of parametric scattering. The inset is a spectral density plot showing the spectrally resolved luminescence for each wave vector, with the theoretical lower branch dispersion overlaid. The pump appears spread in energy and $\mathbf{k}$ due to saturation of the charge-coupled device detector.

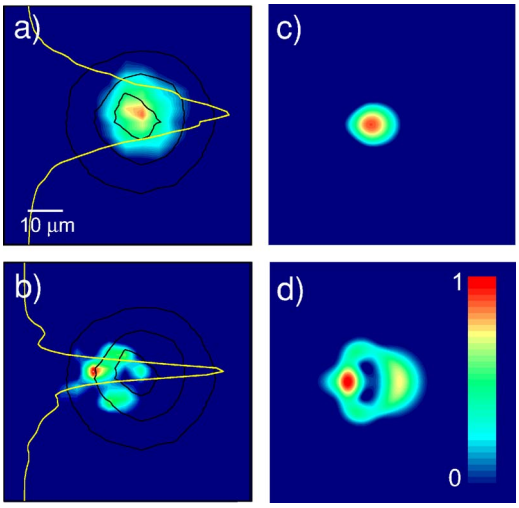

FIG. 2. (Color online) (a) Experimental signal image for pump powers at the threshold (4 mW) for parametric scattering and (b) at 6 times the threshold. (c) Simulated signal distribution at threshold and (d) at 1.5 times the threshold. The pump beam is ~30 μm in diameter, and is incident from the right along the horizontal axis. The black contours on (a) and (b) indicate the near-Gaussian profile of the pump beam, as determined by the photoluminescence at low powers (0.1 mW). Linescans across the signal image in the vertical direction are shown by yellow lines (gray in the printed version). Linear color scale (gray scale on printed version) in (d) refers to all the spatial images of Figs. 2–4.

In Figs. 2(a) and 2(b) spatial images of the signal obtained for laser powers of 4 and 24 mW are shown, corresponding, respectively, to pump powers at the threshold and 6 times the threshold power for the stimulated parametric process. At the threshold, strong narrowing of the polariton emission spectrum occurs, the signature of the formation of the coherent signal state at $\mathbf{k}=0$.[3] The photoluminescence image below the threshold is superimposed as black contour lines in Figs. 2(a) and 2(b); the near-Gaussian spot has FWHM of ~30 μm (the central contour shown). At threshold, where line narrowing and the onset of nonlinear behavior is observed, narrowing of the emission region to 18 μm occurs [see the line scan across the image of Fig. 2(a)]. Increasing the intensity of the pump beam to 6 times the threshold [Fig. 2(b)], the signal emission becomes very asymmetric with a pronounced shift parallel to the direction of the incident laser beam, which is incident from the right of the figure, and shows marked regions of localized polariton emission, with typical FWHM of 6 μm [see the linescan across Fig. 2(b)]. It is important to note that the most intense region of the pump spot (its center) is now depleted with very little signal emission seen.

Theoretical images were calculated using the numerical method described in Ref. 17. The dynamics are simulated in the time domain, with coupled cavity and exciton fields defined on a two-dimensional spatial grid. The model includes the dispersions of the two fields, so that diffractive effects are accounted for, and the exciton mode is given a local $\chi^{(3)}$ nonlinearity of the form $|\phi|^2\phi$, where ϕ is the exciton amplitude. The $\chi^{(3)}$ nonlinearity gives rise to the self-interaction term or blueshift, which is very important in determining the OPO dynamics. Time sequences of data are calculated and stored, then Fourier-transformed to separate the pump, signal, and idler modes. The images show the polariton intensity inside the cavity; the external emission pattern is additionally modified by the polariton dispersion, which, close to $\mathbf{k}=0$, causes an additional broadening of order $\hbar(M_p\gamma)^{-1/2}$, where M_p is the polariton effective mass ($\sim 3\times 10^{-5} m_e$), and γ its linewidth. This corresponds to approximately 5 μm for the experimental cavity parameters. The equivalent effect for the pump light entering the cavity is included in the model, in the way that the cavity mode is driven.

The simulations of the OPO signal at and above the threshold are shown in Figs. 2(c) and 2(d). At the threshold [Fig. 2(c)], the numerical simulation shows good agreement with the experimental picture [Fig. 2(a)] as expected, showing a buildup of the signal in a small region around the center of the laser spot. The theoretical image, at 1.5 times the threshold in Fig. 2(d), shows a central region with depleted signal emission, with the maximum intensity shifted along the pump direction, as observed experimentally in Fig. 2(b). However, the theoretical image shows a ringlike shape and does not account for the localized polariton regions of the experimental counterpart. Moreover, at higher pump powers (typically above ~3 times the threshold value), the numerical model does not settle down into a steady state; the OPO polariton signal becoming unstable.

The general features of the theoretical images can be understood using an analytical model we have developed to describe the microcavity OPO under uniform illumination, taking into account all (i.e., pump, signal, and idler) contributions to the blueshift.[16] This model shows that the OPO state only stays switched on for a finite range of pump powers; there is a lower threshold at which the parametric scattering is strong enough to overcome the losses in the signal and idler modes, but also an upper limit, where the signal and idler blueshift contributions push the system away from resonance, forcing it to switch off. Thus, for pump powers close to threshold, the threshold power density is reached only near the center of the beam, and the OPO spot is small. This effect is clearly shown in Figs. 2(a) and 2(c). At higher powers, however, the upper threshold is crossed at the center of the pump beam, switching the OPO off, while further toward the periphery of the beam profile, the power becomes sufficient to activate the parametric scattering. This effect causes the ringlike form of the image in Fig. 2(d). At the same time a visible asymmetry builds up in the direction of the $\mathbf{k}$ vector of the incident pump. This effect is driven by diffraction due to the finite pump wave vector, which even in the linear regime makes the polariton spot asymmetric and shifted slightly away from the beam center. However, the nonlinear scattering greatly amplifies the asymmetry in the OPO.

The clearest difference between the experimental and theoretical images of Figs 2(b) and 2(d) is the presence of localized regions of polariton emission in Fig. 2(b). We now demonstrate below that these arise from lateral fluctuations in the photonic potential in the samples. Figures 3(a) and 3(b) show the signal emission pattern for another spot on the sample at powers in the coherent regime at 6 times the threshold as in Fig. 2(b), but with opposite incident pump

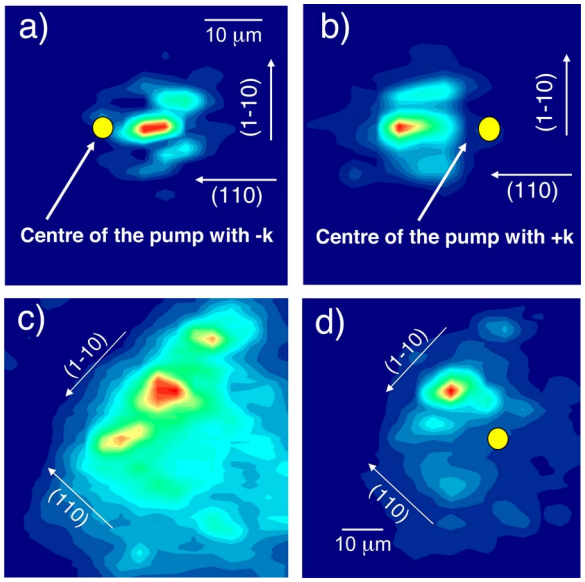

FIG. 3. (Color online) Images of the OPO signal at powers 6 times above the threshold for a pump incident from the left (a) and the right (b) of the sample. (c) Polariton emission for a pump at threshold but with a bigger spot size (FWHM ~50 μm), incident at 45° relative to the [110] and [1$\bar{1}$0] directions. (d) Same as (c) but 2.5 times above the threshold. The signal is strongly confined in the regions of the deepest photonic potential.

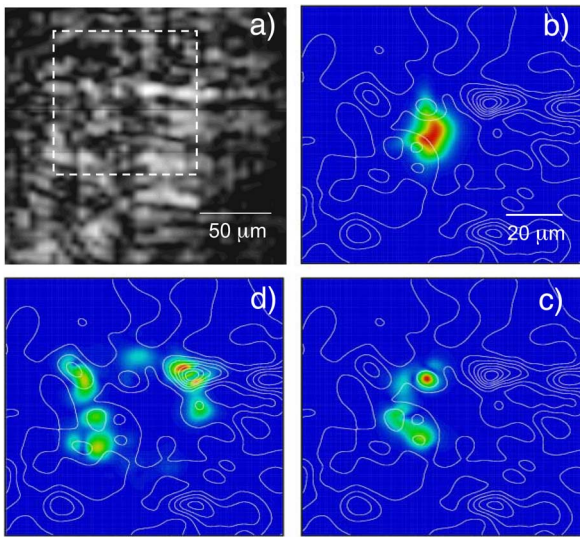

FIG. 4. (Color online) (a) 2D spatial images of the microcavity transmission at the energy of the cavity resonance. Bright and dark regions correspond to lower and higher transmission of the microcavity, respectively. (b) and (c) spatial images of the calculated signal emission with a 30 μm spot size. (b) just above the threshold and (c) at 5 times the threshold. (d) 50 μm pump spot for the same peak power as (c). The background white contours represent a digitized representation of the photonic potential of the selected 100 $\times$ 100 μm^2 dashed region in (a).

directions. The signal is seen to be shifted from the center of the pump beam (yellow spot) in opposite directions along the pump **k** vector in each case, as predicted by the theory. In addition, there is partial alignment of the emission regions along the principal crystallographic axes ([110] and [1$\bar{1}$0]) of the sample. To support this observation we rotated the sample by 45°, and employed a pump spot approximately a factor of 2 larger than for Figs. 2(a) and 2(b) to span more of the disorder. In Fig. 3(c), with the pump power at the threshold, alignment of the localized spots is seen along the [110] and [1$\bar{1}$0] directions, further accentuated at 2.5 times the threshold in Fig. 3(d).

To investigate the nature of the fluctuations giving rise to the localization in the polariton distribution, we measured two-dimensional images of the cavity transmission using a narrow-linewidth laser in resonance with the bottom of the lower polariton branch. The result is shown in Fig. 4(a). The cavity transmission is found to be modulated by partially ordered fluctuations in the photonic potential, with preferential alignment along the [110] and [1$\bar{1}$0] directions. Both the observed separation of the maxima in transmission of 10–20 μm, and the preferential alignment are in good agreement with the patterning seen in the signal images of Figs. 2 and 3. Detuning the laser wavelength by 300–400 μeV resulted in a reversal of the spatial contrast of the image (not shown). These observations show that polaritons in the cavity experience partially ordered local variations in the photonic potential of a few hundred μeV, in potential wells of ~5–10 μm size, with ~10–20 μm separation. We have obtained similar transmission images on several different MOCVD grown wafers.[18] Moreover, previous studies using resonant Rayleigh scattering[19–21] have shown evidence for [110], [1$\bar{1}$0] oriented disorder in microcavities, suggested to arise from the lattice relaxation in the strained Bragg mirrors. We have recently observed that the cavity mode is inhomogeneously broadened in high-Q cavities, on length scales of 10 μm.[22] These results suggest that spatial inhomogeneities in the cavity energy of the type reported in Fig. 4(a) are a characteristic feature of presently available high-Q factor GaAs-based microcavities.

Simulations of the spatial distribution of the signal as in Figs. 2(c) and 2(d) were carried out, but now including a disordered photonic potential derived from the transmission image, using a representative region of 10^4 μm^2 from Fig. 4(a) (dashed area). The results are shown in Figs. 4(b)–4(d), for a pump incident from the right (as in Fig. 2). A pump spot size of 30 μm is employed for Figs. 4(b) and 4(c) and 50 μm for Fig. 4(d). Compared to the results of Figs 2(c) and 2(d), extra structure in the images arises, due to a preferential scattering to minima in the photonic potential, where the phase-matching condition is best satisfied. Figure 4(b), at the threshold shows a near circular spot, similar to Fig. 2(c). At 5 times higher power in Figs. 4(c) and 4(d), strong signal localization is observed in regions of minima of the photonic potential (shown by the background contours). In Fig. 4(c) (30 μm pump spot), the ringlike structure similar to Fig. 2(d) is visible, but strongly modulated by the photonic potential, with bright spots occurring at regions of optimum phase matching. Both the depletion around the pump spot center, and the clear localization found in the experimental images of Figs. 2(b), 3(a), and 3(b) are reproduced well. In Fig. 4(d) with a 50 μm spot, phase matching over a significantly

wider region is seen, in accord with the images of Figs. 3(c) and 3(d), with indications of [110] alignment now visible, as seen experimentally. In both Figs. 4(c) and 4(d) the spot is stable, while without the photonic potential the images are highly unstable at these powers.

In conclusion, the spatial distribution of a macroscopically occupied coherent polariton state generated by stimulated parametric scattering has been observed and modeled. By comparison with numerical simulations, we have shown that the pattern formation is, in part, an intrinsic property of the OPO, due to the nonlinear blueshift, and partly from fluctuations in the photonic potential in the cavity. Minima in the fluctuations act as local phase-matching condition regions for parametric scattering and lead to the formation of a stable signal state. Since disorder in the structure is at present unavoidable in semiconductor microcavities, we conclude that the behavior of polaritons cannot be studied without considering the effects on a local scale. On the other hand, the spatial localization of polaritons may be advantageous for the occurrence of bosonic condensation phenomena. It remains an open question whether, in a spatially invariant cavity with more uniform illumination, structure due to spatial instabilities (e.g., solitons or vortices) will be found. Numerical simulations of this situation suggest that, depending on the pump power, both homogeneous and patterned emission spots may occur.

This work was supported by the EPSRC, Grant No. GR/S09838/01. We thank W. Langbein for helpful discussions on periodic modulation of transmission in microcavities.

*Electronic address: d.sanvitto@shef.ac.uk

[1] M. S. Skolnick, A. I. Tartakovskii, R. Butté, and D. M. Whittaker, IEEE J. Sel. Top. Quantum Electron. **8**, 1060 (2002).

[2] P. G. Savvidis, J. J. Baumberg, R. M. Stevenson, M. S. Skolnick, D. M. Whittaker, and J. S. Roberts, Phys. Rev. Lett. **84**, 1547 (2000).

[3] R. M. Stevenson, V. N. Astratov, M. S. Skolnick, D. M. Whittaker, M. Emam-Ismail, A. I. Tartakovskii, P. G. Savvidis, J. J. Baumberg, and J. S. Roberts, Phys. Rev. Lett. **85**, 3680 (2000).

[4] A. I. Tartakovskii, D. N. Krizhanovskii, and V. D. Kulakovskii, Phys. Rev. B **62**, R13298 (2000).

[5] C. Ciuti, P. Schwendimann, B. Deveaud, and A. Quattropani, Phys. Rev. B **62**, R4825 (2000).

[6] C. Ciuti, P. Schwendimann, and A. Quattropani, Phys. Rev. B **63**, 041303(R) (2001).

[7] D. M. Whittaker, Phys. Rev. B **63**, 193305 (2001).

[8] N. A. Gippius, S. G. Tikhodeev, V. D. Kulakovskii, D. N. Krizhanovskii, and A. I. Tartakovskii, Europhys. Lett. **67**, 997 (2004).

[9] P. G. Lagoudakis, P. G. Savvidis, J. J. Baumberg, D. M. Whittaker, P. R. Eastham, M. S. Skolnick, and J. S. Roberts, Phys. Rev. B **65**, 161310(R) (2002).

[10] A. Baas, J.-P. Karr, M. Romanelli, A. Bramati, and E. Giacobino, Phys. Rev. B **70**, 161307(R) (2004).

[11] W. Langbein, Phys. Rev. B **70**, 205301 (2004).

[12] A. Baas, J. P. Karr, H. Eleuch, and E. Giacobino, Phys. Rev. A **69**, 023809 (2004).

[13] J. P. Karr, A. Baas, R. Houdré, and E. Giacobino, Phys. Rev. A **69**, 031802(R) (2004).

[14] H. Deng, G. Weihs, D. Snoke, J. Bloch, and Y. Yamamoto, Proc. Natl. Acad. Sci. U.S.A. **100**, 15318 (2003).

[15] M. Richard, J. Kasprzak, R. André, R. Romestain, L. S. Dang, G. Malpuech, and A. Kavokin, Phys. Rev. B **72**, 201301(R) (2005).

[16] D. M. Whittaker, Phys. Status Solidi C **2**, 733 (2005).

[17] D. M. Whittaker, Phys. Rev. B **71**, 115301 (2005).

[18] W. Langbein has observed (110) patterning in transmission images for MBE grown cavities, 2004 (private communication).

[19] R. Houdré, C. Weisbuch, R. P. Stanley, U. Oesterle, and M. Ilegems, Phys. Rev. Lett. **85**, 2793 (2000).

[20] M. Gurioli, F. Bogani, D. S. Wiersma, P. Roussignol, G. Cassabois, G. Khitrova, and H. Gibbs, Phys. Rev. B **64**, 165309 (2001).

[21] M. Gurioli, F. Bogani, L. Cavigli, H. Gibbs, G. Khitrova, and D. S. Wiersma, Phys. Rev. Lett. **94**, 183901 (2005).

[22] D. Sanvitto, A. Daraei, A. Tahraoui, M. Hopkinson, P. W. Fry, D. M. Whittaker, and M. S. Skolnick, Appl. Phys. Lett. **86**, 191109 (2005).